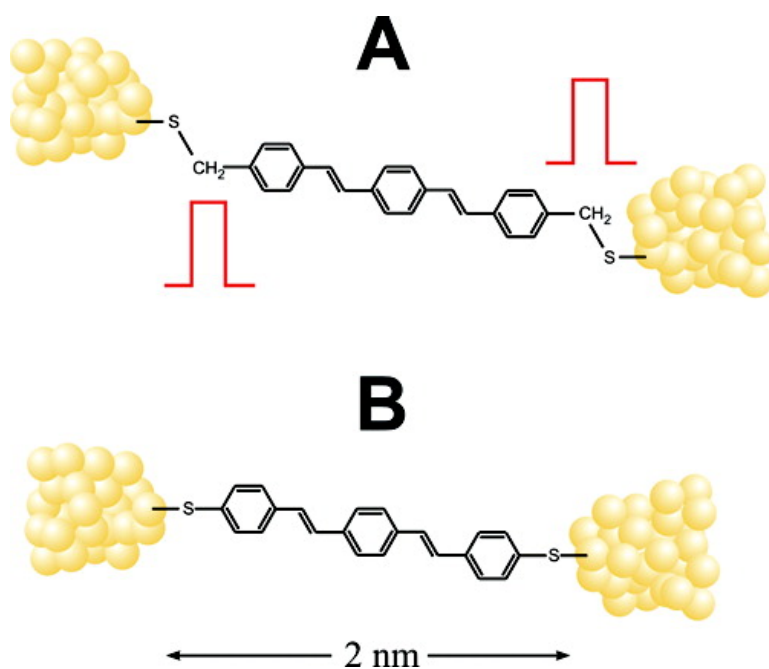


Electronic Transport in Single Molecule Junctions: Control of the Molecule-Electrode Coupling through Intramolecular Tunneling Barriers

Andrey Danilov, Sergey Kubatkin, Sergey Kafanov, Per Hedegrd, Nicolai Stuhr-Hansen, Kasper Moth-Poulsen, and Thomas Bjrnholm

Nano Lett., 2008, 8 (1), 1-5 • DOI: 10.1021/nl071228o • Publication Date (Web): 18 December 2007

Downloaded from <http://pubs.acs.org> on April 30, 2009



More About This Article

Additional resources and features associated with this article are available within the HTML version:

- Supporting Information
- Links to the 5 articles that cite this article, as of the time of this article download
- Access to high resolution figures
- Links to articles and content related to this article
- Copyright permission to reproduce figures and/or text from this article

[View the Full Text HTML](#)



ACS Publications
High quality. High impact.

NANO LETTERS

Electronic Transport in Single Molecule Junctions: Control of the Molecule-Electrode Coupling through Intramolecular Tunneling Barriers

Andrey Danilov,^{†‡} Sergey Kubatkin,[‡] Sergey Kafanov,[‡] Per Hedegård,[†] Nicolai Stuhr-Hansen,[†] Kasper Moth-Poulsen,[†] and Thomas Bjørnholm^{*†}

Nano-Science Center (Niels Bohr Institute and Department of Chemistry), University of Copenhagen, Universitetsparken 5, DK-2100 Copenhagen, Denmark, and Department of Microtechnology and Nanoscience, Chalmers University of Technology, S-41296 Göteborg, Sweden

Received May 24, 2007; Revised Manuscript Received November 8, 2007

ABSTRACT

We report on single molecule electron transport measurements of two oligophenylenevinylene (OPV3) derivatives placed in a nanogap between gold (Au) or lead (Pb) electrodes in a field effect transistor device. Both derivatives contain thiol end groups that allow chemical binding to the electrodes. One derivative has additional methylene groups separating the thiols from the delocalized π -electron system. The insertion of methylene groups changes the open state conductance by 3–4 orders of magnitude and changes the transport mechanism from a coherent regime with finite zero-bias conductance to sequential tunneling and Coulomb blockade behavior.

With the aim to reveal the fundamental structure–property relations for electron transfer between a molecule and a metal electrode at the single molecule level, electronic transport through single π -conjugated molecules has been addressed in a number of recent experimental^{1–19} and theoretical^{20–25} papers. In the present paper, we address key issues concerning the relation between electronic transport and the strength of the electronic coupling between molecule and electrode by measuring the charge transport properties of single molecules connected to source and drain electrodes while

electrostatically influenced by a third so-called gate electrode. If weakly coupled to the leads, the charge transport is expected to occur in a stepwise process where a unit charge first tunnels onto the molecule and, after a residence time allowing relaxation to the ground state of the charged molecule, tunnels on to the drain electrode in a second step. While residing on the molecule the charge prevents further charges to transfer to the molecule due to Coulomb charging. The Coulomb blockade can be lifted by tuning the gate electrode potential, resulting in an open state with a typical resistance of $\approx 1 \text{ G}\Omega$.⁴ In the opposite so-called strong-coupling regime, the electronic states on the molecule and

* To whom correspondence should be addressed. E-mail: tb@nano.ku.dk.

[†] University of Copenhagen.

[‡] Chalmers University of Technology.

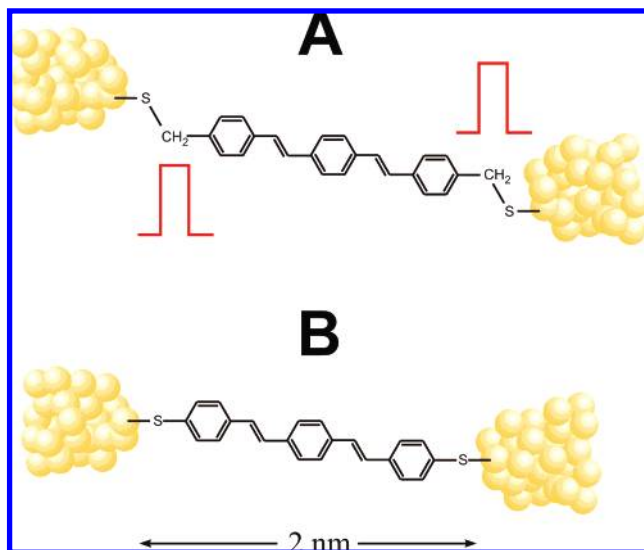


Figure 1. Schematic representation of molecules **A** and **B** placed in electrode gaps. Derivative **A** has an extra methylene ($-\text{CH}_2-$) group inserted between sulfur and the π -conjugated moiety, providing a tunneling barrier (shown in red).

electrode are significantly hybridized leading to coherent tunneling process transferring charge in one step from the source to the drain electrode. The Coulomb blockade in this case is washed out by quantum fluctuations of the molecular charge, and the molecular resistance can be of the order of the resistance quantum $R_0 = 25.8 \text{ k}\Omega$.²⁶

Our experimental strategy to test the molecule–electrode coupling has been to study two very similar molecules which both contain the OPV3 electronic moiety capped with acetyl protected thiol groups allowing a chemical bond to be formed to a gold electrode (Figure 1, molecules **A** and **B**). The insertion of a methylene ($-\text{CH}_2-$) group between the thiol and the benzene ring in **A** provides a chemically defined tunneling barrier,⁹ and the electronic coupling between OPV3 and electrode is hence expected to be significantly smaller for **A** than **B**. In a previous study, we used tertiary butyl protected thiol end-capped OPV5 molecules⁴ which also provide a tunneling barrier between the π -conjugated molecule and the electrodes. The OPV5 derivative from ref 4 and **A** from the present study are hence both expected to couple weakly to the metal electrode, whereas **B** can couple strongly.

The molecules were placed in an $\sim 2 \text{ nm}$ gap between gold electrodes as described in detail in previous publications.^{4,6,11,15} First, gold is evaporated in UHV at 4 K on to an aluminum oxide covered aluminum gate electrode through a mask elevated above the surface. The resulting tunneling gap is carefully characterized.^{6,27,28} In a subsequent step, a second evaporator allows the molecules to be sublimated through the same mask typically in a submonolayer coverage ($\sim 1\%$). At 4 K, the molecules are stuck at the sites where they initially contact the aluminum oxide surface. After completion of the molecule deposition, the $I-V$ characteristic of the gap is unchanged indicating that no molecules have evaporated directly into the gap. In the last step, molecules are trapped in the gap by applying a bias across the gap while annealing at about 30–50 K. The combination of electrostatic

Table 1. Summary of Transport Properties for All Devices Measured^a

Molecule A		
device	$R_{\text{open state}} (\text{M}\Omega)$	$E_{\text{add}} (\text{eV})$
1	3500	0.722
2	3000	0.766
3	400	0.760
4	230	0.686
4'	230	0.928
Molecule B		
device	$dV/dI (\text{M}\Omega)_{\text{at bias } 50 \text{ mV}}$	transport gap (eV)
5	5.6–6.4	
6	4.2–5.8	
7*	3.7–3.8	
8	1.6	
9*	2.3	
10*	17–53	
11	23	
12	2.4	
13	0.34–0.38	
14	0.43–0.55	
15	0.33–0.51	
16	0.49	0.9

^a Device 4 had lead electrodes, and all other devices had gold electrodes. Two complete Coulomb diamonds were traced for device 4, and their parameters are presented separately in lines 4 and 4'. For devices with molecule **B** the symbol * marks the ones where a weak gate modulation was observed (see Figure 2c for example); all other devices had no measurable gate effect. Some devices changed their conductivity after moderate annealing (up to 20 K) or were switching between different conductance states, as explained in ref 15. For switching devices both upper and lower resistance limits are presented. The indicated dV/dI are for the transport bias 50 meV. We recorded $I-V$ curves at higher biases until the device was burned. Only device 16 (Figure 2d) was measured at high enough bias to estimate the transport gap of $\sim 1 \text{ eV}$ which is comparable to break junction measurements.

attraction to the gap and thermally induced mobility of molecules allow the individual and largely separated molecules deposited on the aluminum oxide surface to diffuse into the gap. Once a molecule is trapped, a dramatic change in the current flowing across the gap is observed. At this point, the device is cooled back to 4 K, and detailed measurements are performed at this temperature. Altogether four devices with molecule **A** and 12 devices with molecule **B** were fabricated. All fabricated devices are included in the present paper and no deliberate picking from a bigger pool of data was done. All devices with the same molecule showed similar characteristics revealing good reproducibility of the data (Table 1). In all cases, the thiol end groups were protected with acetyl thiols which are known to allow stable bonding to gold surfaces.²⁹ Overall resistances of devices with molecule **A** are consistently in the $\text{G}\Omega$ range, whereas junctions with molecule **B** show typical resistances about 0.2–1 $\text{M}\Omega$. The latter values are similar to values obtained in break junction measurements of similar deprotected thiol end-capped molecules.^{7,30} Therefore, we assume that the thiol is chemically bound to both gold electrodes in these most conducting junctions. Table 1 also lists examples with the same molecule **B** but with lower overall conductance. These may represent situations where the molecule is strongly coupled to one side but not to the other. The actual bonding

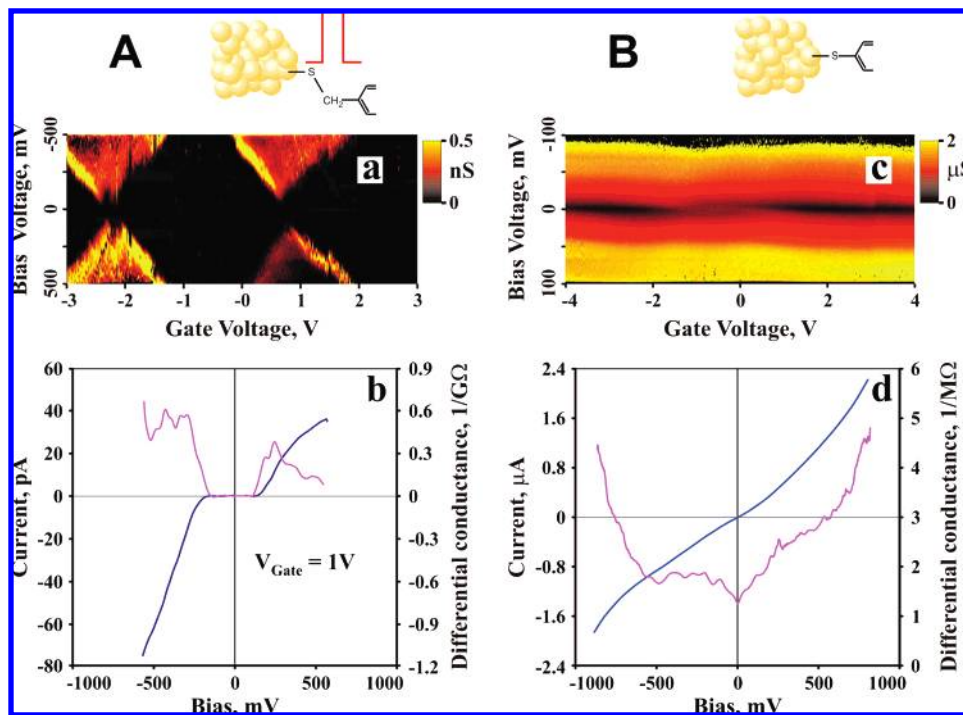


Figure 2. Comparison of electron transport characteristics of OPV3 molecules **A** (left) and **B** (right). (a) Differential conductance (color code) vs the gate and bias voltages for the device 2. (b) Representative $I(V)$ curve (blue) and corresponding dI/dV (magenta) for the same device. (c) weak gate modulation observed for device 10. Note different conductance scale for a and c. (d) Large bias $I(V)$ curve (blue) and corresponding dI/dV (magenta) for device 16. The high bias $I(V)$ was successfully measured for device 16 only. In all other devices an attempt to trace an $I(V)$ curve at biases ± 1 V burned the sample.

process is very likely to be aided by charge transport through the molecule at high source-drain bias as discussed elsewhere.¹⁵

Here we focus on the influence of the OPV–electrode interaction on transport by direct comparison of molecules **A** and **B**. A representative plot of differential conductance vs the gate and bias voltages of molecule **A** is shown in Figure 2a. It has the characteristic diamond shaped form with sharp borders between open (colored) and closed (black) states, providing clear evidence of the typical pattern seen for sequential tunneling through an island with weak coupling to the source and drain electrodes. From this so-called stability diagram, the addition energy $E_{\text{add}} = E_{N+1} + E_{N-1} - 2E_N$, where N is the number of electrons on the molecule, can be determined. It equals the vertical distance in energy from zero to the diamond vertex or equivalently the horizontal distance between two adjacent open states normalized by the strength of the electrostatic gate coupling to the molecule (denoted C_g/C_Σ). For all three samples prepared with gold electrodes, both the positions of the open states in the gate voltage and the vertical diamond sizes were reproducible within a narrow experimental error. The estimates of $E_{\text{add}}(\mathbf{A})$ for five distinct diamonds all lie between 0.7 and 0.9 eV (Table 1).

Previous measurements⁴ on the longer OPV5 derivative reveal E_{add} values between 0.1 and 0.3 eV showing an interesting influence of the length of the π -conjugated system on the addition energy. A priori, one would expect two contributions to this size effect: One of quantum mechanical origin reflecting the increase in the level spacing with

decreasing length and one electrostatic contribution that increases the charging energy for the shorter molecule. From simple model considerations,³¹ one would expect that both contributions are proportional to $1/L$ where L is the length of the π -conjugated system. As a zero order approximation, one finds that $E_{\text{add}} \approx 1 \text{ eV}/L$ with L measured in nanometers is in rough agreement with the two data points ($L_{\text{OPV3}} \approx 1.7 \text{ nm}$ and $L_{\text{OPV5}} \approx 3.2 \text{ nm}$). More elaborate estimates of this size effect are part of a forthcoming paper.³²

To study the effects of the electrode material on the molecular device properties, we substituted the gold (Au) electrode material with lead (Pb) and studied two devices with molecule **A**. The lead electrodes were prepared and characterized in the same way as described above for the gold electrodes. The measurements on molecule **A** inserted between lead electrodes showed similar charging energies but different open state gate voltages as compared to the gold electrodes (Figure 3). Two more samples with lead electrodes were fabricated. These samples were measured at low biases only because attempts to trace stability diagrams at high-biases burned the samples. The diamond sizes (charging energies) were measured directly only for sample 4 listed in Table 1. However, the low bias data do show that the gate voltages corresponding to open states of the transistor are the same for all three samples with lead electrodes.

To summarize, all four devices with molecule **A** demonstrated sequential tunneling with characteristic addition energies of 0.7–0.9 V.

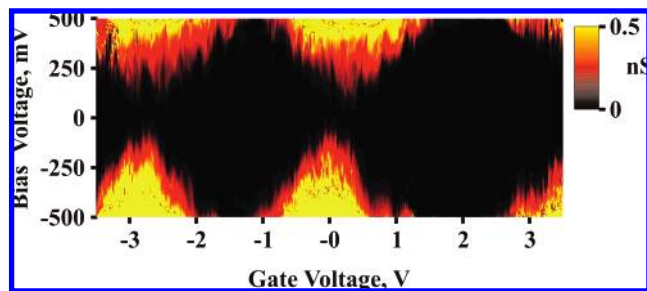


Figure 3. Electron transport characteristics of molecule **A** inserted between lead electrodes. Note similar charging energies but different open state gate voltages as compared to the gold electrodes (Figure 2). In particular, an open state at the gate voltage -2.6 V separates the same charge states as the open state at $+0.8$ V on Figure 2 (see the main text for details).³⁵

When **B** is investigated by the same procedure (Figure 2c,d), the conductance plot is substantially different from the one shown in Figure 2a,b. First of all, the conductance level for the open state has increased by 2–4 orders of magnitude and the gate dependence has become very weak (three samples) or absent (nine samples) (see Table 1). Figure 2d shows a representative I – V curve for a device possessing an overall conductance level similar to that of devices fabricated by break junctions with a comparable thiol end-capped π -conjugated system (cf. refs 7, 29, and 30). The observed weak or no gate effect is direct evidence of a strong coupling of molecular orbitals to the source/drain electrodes. Similar behavior is observed in independent experiments performed in Delft where the vibrational fine structure further provides an independent identification of the molecule in the gap.¹⁶

All devices with molecule **B** have been subjected to spectroscopic measurements at high biases. Only one device with the lowest overall conductance has survived this procedure, and corresponding data are presented in Figure 2d. The high bias sweeps for molecule **B** (± 1.5 V) reveal a ~ 1.6 eV wide transport gap in the tunneling density of states (DOS \approx differential conductance). The differential conductance plot has quantitative agreement with the theoretical calculations of Crlen et al.,²³ where the charge transport through the same molecule symmetrically coupled to gold electrodes was considered. In contrast to the case of strong asymmetric coupling, where the expected transport gap equals the HOMO–LUMO gap in molecular spectrum (3.6 eV for OPV3), for symmetrically coupled molecule the transport gap is reduced to twice the distance from the Fermi energy in the leads to the closest molecular orbital: HOMO or LUMO. This transport gap reduction is due to a strong bias dependence of position of the HOMO level with respect to the electrodes in a self-consistent potential of the metal–molecule junction.^{33,34}

According to the calculations presented in ref 23, the rather strong increase in conductance as the bias approaches ± 0.8 V arises when the Fermi energy in source or drain electrode is aligned with the tail of the HOMO level in OPV3. We note that our data are in good agreement with this calculation both with regard to the magnitude of conduction and the size of apparent transport gap.

The device fabrication procedure ensures that in all devices molecule **B** is chemically bonded to at least one of the electrodes. The absence of the Coulomb blockade also proves that at least one of the molecule–electrode contacts is well coupled (so that the charge fluctuations through this contact destroys charge quantization on the molecule as it was explained in the introduction). The coupling in the second contact may vary from device to device. The device presented in Figure 2d had the highest conductance among all of the devices measured, corresponding to the theoretical result for two chemically bonded contacts. This device was the only device that was not harmed at high biases, strongly indicating that chemical bonds to both sides make the contact more stable.

The presented data substantially extend and corroborate previous observations of the effects of methylene spacer groups on the electron transport from STM,⁹ break-junctions,^{7,30} cross-bar devices,³⁶ and nanoelectrodes.¹⁷ The STM data reported in ref 9 show that the apparent height of the OPV2 molecule is 0.5 Å higher than the height of the derivative with methylene spacer groups, both derivatives being imaged at constant current mode. Since the OPV2 molecule is physically 1.3 Å shorter than the methylene spacer substituted derivative,³⁷ we conclude that the presence of the methylene spacer reduces the tip to molecule gap so that the difference in the tip-to-molecule distance between the two molecules is $\delta = 1.8$ Å. In turn this corresponds to a conductance difference between the two molecules of $e^{-\delta\beta} \approx 100$ times where $\beta \approx 2.5$ Å⁻¹ is the tunneling decay constant for vacuum. The agreement with the present study is good.

In summary, we have provided straightforward experimental evidence showing the significant influence of a single methylene group inserted between the molecular π systems and the metal electrodes. The transport mechanism changes from coherent tunneling to the Coulomb blockade regime, and the sample resistance in the open state increases by several orders of magnitude. The present result is the first direct observation of these effects in a three terminal device and may serve as a central reference point for designing molecules with prescribed transport properties.

Acknowledgment. The work was supported in part by the European Commission through Project FP6-003673 CANEL of the IST Priority. (The views expressed in this publication do not necessarily reflect the official European Commission’s view on the subject.) Funding from the Danish Research Councils and the Danish Nanotechnology Program and Swedish SSF and VR is gratefully acknowledged.

References

- (1) Zhitenev, N. B.; Meng, H.; Bao, Z. *Phys. Rev. Lett.* **2002**, *88*, 226801.
- (2) Park, J.; Pasupathy, A. N.; Goldsmith, J. I.; Chang, C.; Yaish, Y.; Petta, J.R.; Rinkoski, M.; Sethna, J. P.; Abruna, H. D.; McEuen, P.L.; Ralph, D. C. *Nature* **2002**, *417*, 722–725.
- (3) Zhitenev, N. B.; Erbe, A.; Meng, H.; Bao, Z. *Nanotechnology* **2003**, *14*, 254.
- (4) Kubatkin, S.; Danilov, A.; Hjort, M.; Cornil, J.; Brédas, J.-L.; Stuhr-Hansen, N.; Hedegård, P.; Bjørnholm, T. *Nature* **2003**, *425*, 698.
- (5) Mayor, M.; Weber, H. B.; Reichert, J.; Elbing, M.; von Hanisch, C.; Beckmann, D.; Fischer, M. *Angew. Chem., Int. Ed.* **2003**, *42*, 5834–5838.

- (6) Kubatkin, S.; Danilov, A.; Hjort, M.; Cornil, J.; Brédas, J.-L.; Stuhr-Hansen, N.; Hedegård, P.; Bjørnholm, T. *Curr. Appl. Phys.* **2004**, *4*, 554.
- (7) Xiao, X. Y.; Xu, B. Q.; Tao, N. J. *Nano Lett.* **2004**, *4*, 267.
- (8) Zhitenev, N. B.; Erbe, A.; Bao, Z.; Jiang, W. R.; Garfunkel, E. *Nanotechnology* **2005**, *16*, 495.
- (9) Moth-Poulsen, K.; Patrone, L.; Stuhr-Hansen, N.; Christensen, J. B.; Bourgoin, J.-P.; Bjørnholm, T. *Nano Lett.* **2005**, *5*, 783.
- (10) Picciotto, A.; Klare, J. E.; Nuckolls, C.; Baldwin, K.; Erbe, A.; Willett, R. *Nanotechnology* **2005**, *16*, 3110.
- (11) Danilov, A. V.; Kubatkin, S. E.; Kafanov, S. G.; Bjørnholm, T. *Faraday Discuss.* **2006**, *131*, 337–345.
- (12) van der Zant, H. S. J.; Kervennic, Y. V.; O’Niell, K.; de Groot, Z.; Thijsen, J. M.; Heersche, H. B.; Stuhr-Hansen, N.; Bjørnholm, T.; Vanmaekelbergh, D.; van Walree, C. A.; Jennekens, L. W. *Faraday Discuss.* **2006**, *131*, 347–356.
- (13) Keane, Z. K.; Ciszek, J. W.; Tour, J. M.; Natelson, D. *Nano Lett.* **2006**, *7*, 1518–1521.
- (14) Zhitenev, N. B.; Jiang, W.; Erbe, A.; Bao, Z.; Garfunkel, E.; Tennant, D. M.; Cirelli, R. A. *Nanotechnology* **2006**, *17*, 1272.
- (15) Danilov, A. V.; Kubatkin, S. E.; Kafanov, S. G.; Flensberg, K.; Bjørnholm, T. *Nano Lett.* **2006**, *6*, 2184–2190.
- (16) Osorio, E. A.; O’Niell, K.; Stuhr-Hansen, N.; Nielsen, O. F.; Bjørnholm, T.; Zant, H. S. J. *Adv. Mater.* **2007**, *19*, 281–285. Zant H. S. J. Private communication.
- (17) Liang, T. T.; Naitoh, Y.; Horikawa, M.; Ishida, T.; Mizutani, W. J. *Am. Chem. Soc.* **2006**, *128*, 13720–13726.
- (18) Venkataraman, L.; Klare, J. E.; Nuckolls, C.; Hybertsen, M. S.; Steigerwald, M. L. *Nature* **2006**, *442*, 904–907.
- (19) Seferos, D. S.; Blum, A. S.; Kushmerick, J. G.; Bazan, G. C. *J. Am. Chem. Soc.* **2006**, *128*, 11260–11267.
- (20) Ratner, M. A.; Davis, B.; Kemp, M.; Mujica, V.; Roitberg, A.; Yaliraki, S. *Ann. N.Y. Acad. Sci.* **1998**, *852*, 22–37.
- (21) Taylor, J.; Brandbyge, M.; Stokbro, K. *Phys. Rev. Lett.* **2002**, *89* (13), 138301.
- (22) Nitzan, A.; Ratner, M. A. *Science* **2003**, *300*, 1384–1389.
- (23) Crjjen, Z.; Grigoriev, A.; Wendin, G.; Stokbro, K. *Phys. Rev. B* **2005**, *71*, 165316.
- (24) Remacle, F.; Willner, I.; Levine, R. D. *J. Phys. Chem. B* **2004**, *108*, 18129–18134.
- (25) Grigoriev, A.; Sköldberg, J.; Wendin, G.; Crjjen, Z. *Phys. Rev. B* **2006**, *74*, 045401.
- (26) Averin, D. V.; Likharev, K. K. *Single Electronics: A Correlated Transfer of Single Electrons and Cooper Pairs in Systems of Small Tunnel Junctions*, in *Mesoscopic phenomena in Solids*; North-Holland: New York, 1991.
- (27) Kubatkin, S. E.; Danilov, A. V.; Olin, H.; Claeson, T. *J. Low Temp. Phys.* **2000**, *118*, 307.
- (28) Danilov, A. V.; Golubev, D. S.; Kubatkin, S. E. *Phys. Rev. B* **2002**, *65*, 125312.
- (29) Tour, J. M.; Jones, L.; Pearson, D. L.; Lamba, J. J. S.; Burgin, T. P.; Whitesides, G. M.; Allara, D. L.; Parikh, A. N.; Atre, S. V. *J. Am. Chem. Soc.* **1995**, *117*, 9529–9534.
- (30) Reichert, J.; Ochs, R.; Beckman, D.; Weber, H. B.; Mayor, M.; Löhneysen, H. *Phys. Rev. Lett.* **2002**, *88*, 176804.
- (31) Kuhn, W. *Helv. Chim. Acta* **1948**, *31*, 1780–1799.
- (32) Bjørnholm et al. (in prep).
- (33) Zahid, F.; Paulsson, M.; Datta, S. Electrical Conduction through Molecules. In *Advanced Semiconductors and Organic Nanotechniques*; Morkoc, H., Ed.; Academic Press: New York, 2003.
- (34) Zahid, F.; Paulsson, M.; Polizzi, E.; Ghosh, A. W.; Siddiqui, L.; Datta, S. *J. Chem. Phys.* **2005**, *123*, 064707.
- (35) The lead electrodes at 4 K are superconducting. The energy gap Δ in superconducting electrodes should, in principle, reveal itself on the diamond structure as a spectral lines parallel to the diamond edges and placed $\Delta/e \sim 1$ mV apart from the edges.²⁶ However, the sample was too switchy for these features to be resolved.
- (36) Blum, A. S.; Kushmerick, J. G.; Pollack, S. K.; Yang, J. C.; Moore, M.; Naciri, J.; Shashidhar, R.; Ratna, B. R. *J. Phys. Chem. B* **2004**, *108*, 18124.
- (37) Note that in ref 9 the length of plain OPV2 derivative was mistakenly indicated as 13.9 Å. The correct value is 12.9 Å.

NL071228O